

A Web-based Educational Magnetic Resonance Simulator: Design, Implementation and Testing

Daniel Treceño-Fernández¹ · Juan Calabia-del-Campo² · Miguel L. Bote-Lorenzo¹ · Eduardo Gómez Sánchez¹ · Rodrigo de Luis-García¹ · Carlos Alberola-López¹

Received: 27 Dec 2018 / Accepted: 03 Oct 2019

Abstract A new web-based education-oriented magnetic resonance (MR) simulator is presented. We have identified the main requirements that this simulator should comply with, so that trainees can face useful practical tasks such as setting the exact slice position and its properties, selecting the correct protocol or fitting the parameters to acquire an image. The tool follows the client-server model. The client contains the interface that mimics the console of a real machine and several of its features. The server stores anatomical models and executes the bulk of the simulation. This cross-platform simulator has been used in two real educational scenarios. The acceptance of the tool has been measured using two criteria, namely, the System Usability Scale and the Likelihood to Recommend, both with satisfactory results. Therefore, we conclude that given the potential of the tool, it may play a relevant role for the training of MRI operators and other involved personnel.

Keywords Magnetic Resonance Imaging MRI · Simulator System · Medical training/educational tool · System Usability Scale SUS

1 Introduction

Magnetic Resonance Imaging (MRI) is a non-invasive medical imaging modality commonly used for diagnosis of pathologies related to soft tissue. It is multiparametric modality, which allows the acquisition of a great variety of images by a proper selection of the pulse sequences and its parameters. Consequently, this modality has experienced great growth in recent years as reflected in [1]. However, operating a MRI scanner is not an easy task and several factors contribute to these difficulties. First, the fundamentals of MRI lie on advanced concepts of nuclear physics, electromagnetism and signal processing;

¹University of Valladolid, Valladolid, Spain

²Hospital Clínico Universitario, Valladolid, Spain

second, MRI acquisition heavily depends on a large number of parameters, which should be fine-tuned for optimal quality and, in particular, to avoid the generation of artifacts. Furthermore, clinical demands and high costs imply extensive scanner use, so hands-on sessions for practitioners can hardly be afforded. Hence, the development of computerized simulators for training in MRI seems a solid alternative. If properly designed and implemented, such simulators would provide a deeper understanding of the elements involved, as well as extensive practicing for trainees prior, or in addition, to handling a real scanner.

We will first review the tasks that a technician needs to accomplish for MRI acquisition; then, we will review related work in the field of MRI simulation.

1.1 Overview of the technician operation for MRI acquisition.

The process to be executed by an operator of a magnetic resonance machine consists of two stages, namely, (a) patient preparation and (b) sequence preparation, execution and inspection [2]. The second stage is executed when the technician is in front of the console. The process usually starts by entering patient information, so that properly identified images can be stored and retrieved. Patient position and orientation have to be manually entered. The system should be able to determine the type of antenna that has been connected to the equipment; in any case, the technician should double check that the correct antenna is detected. The protocol, i.e., the list of sequences to be launched, is then defined; parameters are usually pre-determined, but the technician may carry out some adjustments in order either to shorten scan time or to improve contrast. Once this is decided, a survey is launched; this consists of a series of low resolution and large field of view (FOV) images that are used for spatial planning; the number of acquired images may vary, although three images taken in each of the three principal plains (axial, sagittal and coronal) are customary. This set of images is then used to define the location and orientations of the slices to be acquired for each of the sequences; the acquired slices can have arbitrary orientations in space for optimum location of the pathology within the images. In areas such as the heart, planning can involve various acquisitions for the correct orientation of the slices. This is easily carried out by means of a graphical interface, in which the intersections between the slices and the image planes are highlighted in some color, and the technician can move them around in the three dimensions and rotate them at will. Finally, the sequence is launched and the technician is expected, upon termination, to inspect the image quality to double check the absence of artifacts and, if necessary, to repeat any of the acquisitions. The process finishes by saving the reconstructed images, either locally or to the Picture Archiving and Communication System (PACS) [3,4], according to the hospital regulation. Occasionally, some postprocessing is needed (say, for instance, to calculate some specific maps in diffusion sequences [5]); the technician should know this possibility and react accordingly.

1.2 Related work within the field of MRI simulation.

A number of MRI simulators have been proposed in the literature. Early work includes the proposal of basic MRI simulators [6, 7], intended for experimenting with different imaging sequences and basic acquisition parameters. Simulators designed for pulse sequence prototyping were presented in [8, 9], and specific tools were proposed for the simulation of hardware-related artifacts [10, 11], and for the effects of subject motion in some specific sequences [12, 13]. In [14], a tool was proposed to analyze the influence of MRI parameters on acquisition time and contrast. Other tools focus on image reconstruction and postprocessing [15–17], and the effects of time-varying magnetic fields or susceptibility artifacts [18–20]. Some methods have also been implemented for the simulation of MR images incorporating distributions of multiple tissues within a voxel or even multiple compartments [21–23]. Albeit powerful, they are actually software libraries that do not constitute by themselves an educational tool for radiographers.

Among all the aforementioned contributions, only the works in [6, 7] are considered as educational MRI simulators and have been used in training scenarios. The latter, known as Virtual MRI, is a standalone Java applet and covers the steps of parameter selection and image acquisition described in section 1.1. Another tool, known as POSSUM [12, 18–20] is part of FMRIB’s Software Library (FSL) and can produce images of great realism; similarly to Virtual MRI, it focuses on the steps of parameter selection and acquisition but, as opposed to the former, it requires a complete installation of FSL. Realism, on the other side, translates itself in prolonged acquisition times. Finally, MRILab [24] is quite a complete simulator, as it covers coil selection, spatial planning, parameter selection and image acquisition. However, spatial planning is limited to orthogonal slices and to the principal directions and the new simulated acquisitions can not be used for a new spatial planning. It is also constrained by the fact that it only runs in Matlab, and if accelerated simulations are desired, an Nvidia graphics card is mandatory.

Therefore, we have identified the need of a software tool that covers the whole process that a technician performs at the console in the clinical routine. Such a tool, specifically designed for radiographer training, is described in the paper.

2 The MRI Simulator

2.1 System requirements

On the basis of a literature review and interviews with senior radiologists from the Spanish Society of Medical Radiology (SERAM¹), and radiographers and educators from the School of Radiographers of the Hospital Clínico San Carlos, Madrid, Spain, we have identified a set of features that an MRI simulator

¹ <https://www.seram.es/>

designed for radiographer training should possess. Functional requirements are:

- The system should be able to simulate images created from a set of acquisition sequences that constitute a protocol. The user should also be able to create and execute those protocols. Patient positioning and coil selection should also be available.
- The user should be able to change basic acquisition parameters, such as TE (echo time), TR (repetition time) and, where applicable, IR (inversion time), flip angle, ETL (echo train length) and others.
- Geometrical planning should be included in the simulation workflow, from slice orientation to the determination of the FOV (field of view), slice thickness, slice separation, and selection of phase/frequency encoding directions.
- Acquisition artifacts should be generated at trainer demand.
- k-space manipulation should be supported.
- Different educational roles should be supported, allowing trainers to create educational scenarios and trainees to work on those scenarios and report their results.

Non-functional requirements are:

- Short simulation times are needed so that action/reaction is possible in acceptable times for an educational session.
- The system should be easy to access/install and able to work over a wide range of platforms.
- The system will avoid, whenever possible, the specificities associated to each manufacturer as well as to use vendor-associated sequence names.

Based on these requirements, we have opted for a simple simulation model, consisting in evaluating mathematical expressions of sequences which are then corrupted with artifacts, as will be shown in section 2.3.3. Rigorous detailed simulations, as described in section 1, have been avoided to allow a more responsive user experience. How the rest of the requirements are satisfied will be described in this section.

2.2 Architectural design

The system is designed following a client-server architecture; the server, on one side, follows a service-oriented architecture (SOA), where services are (See Fig. 1):

- Static files service, used to serve files that do not require authentication, specifically, all the graphical user interface (GUI) files and the simulated images.
- Authentication service, to give access to users with different roles, as required in section 2.1.
- Simulator data service. It provides the data to the GUI (protocols, anatomical parts, coils, etc. available in the database).

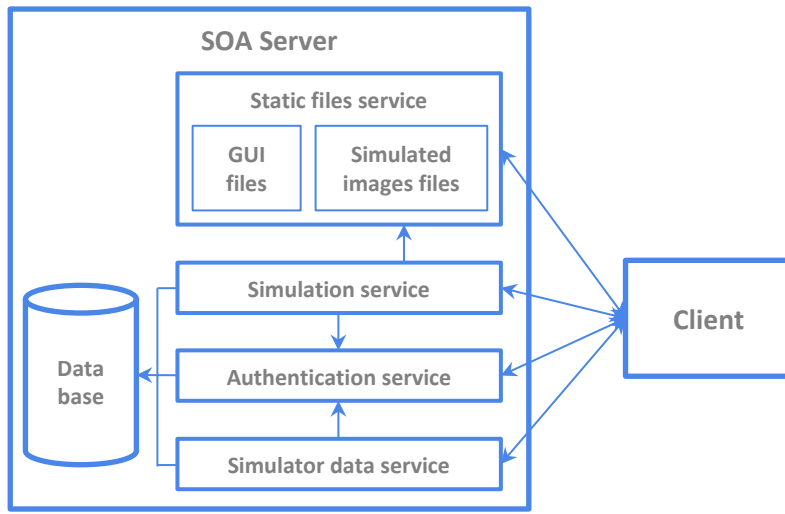


Fig. 1 The server follows a Service-oriented architecture that performs four main tasks: static files service, simulation service, authentication service and simulator data service. Simulation and data services require authentication. With the exception of the static files service, the rest have access to the database.

- Simulation service, that carries out the actual simulation and adds the simulated image to the static files repository.

On the client side, the interface has a component-oriented design, where each interface element consists of one or several components that follow the Model-View-Viewmodel (MVVM) pattern [25].

2.3 Implementation and overview

We have opted for a web application since it does not need installation and is accessible from a browser. The GUI follows the MVVM pattern and has been implemented with AngularJS². GUI content is described in Section 2.3.1. The geometric planning, our most outstanding feature, is described in section 2.3.2.

The server was programmed in Python using the Django framework [26]. The simulations are performed using C++ and the ITK library³; interaction with Python is achieved through a wrapper. The actual simulation is described in section 2.3.3.

The simulation service (Fig. 1) uses the simple object access protocol (SOAP) given the need to exchange rich requests and responses with the client. The remaining services apply a representational state transfer (REST) application program interface (API).

² <https://angularjs.org/>

³ <https://itk.org/>

2.3.1 Interface overview

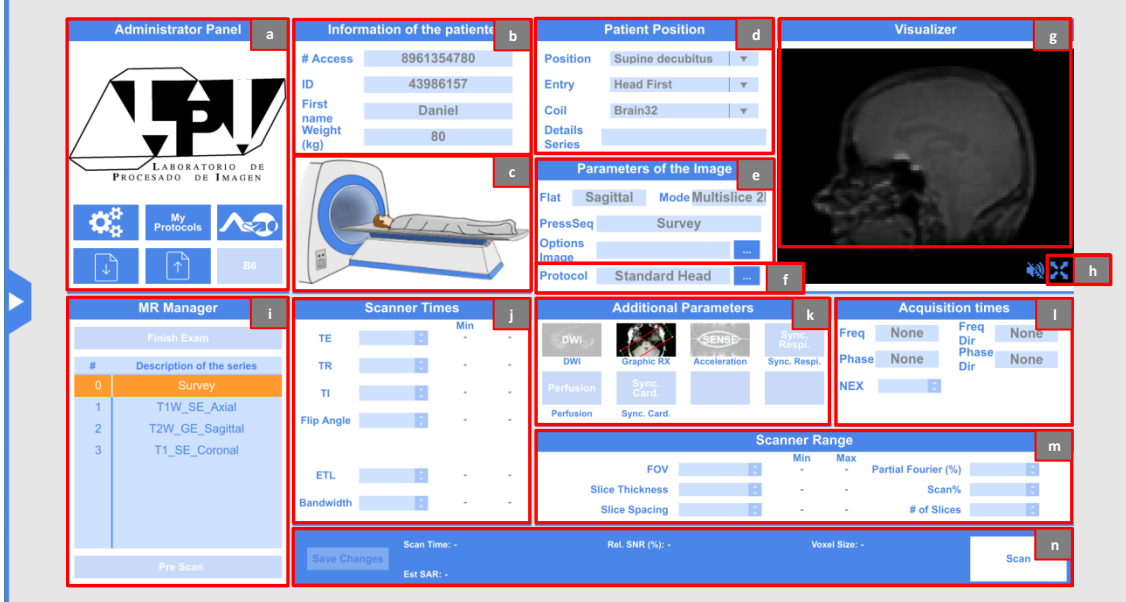


Fig. 2 Simulator main interface. All the characteristics of the simulator will have access from this interface, many of them directly as the patient's information (b), its position (d), the selection of parameters of the sequence (j) and so on. The remaining features may be accessed through buttons such as those located on panels a and k. Superimposed letters are used to guide the explanation in the main text.

The interface design decisions have been made in collaboration with the group of professionals mentioned in Section 2.1, where the basic aspects of the resonance have been taken into account and attempts have been made to be generalists in order to comply with our third non-functional requirement.

The main interface is shown in Fig. 2, where the user needs to: enter patient information (Fig. 2-b); select patient position (Fig. 2-d; when this action is taken, the icon in 2-c will vary accordingly) and coil; select a protocol from a menu that pops when the protocol button is clicked (Fig 2-e). Once selected, the protocol is loaded in Fig. 2-i; this panel contains the information of each of the pulse sequences that make up a certain protocol.

As a rule, for each sequence the user should select the relevant parameters through panels e, j, k, l, m in Fig. 2 and then carry out the appropriate geometrical planning (see Fig. 3). Finally, the scan button should be pressed (Fig. 2-n). At this moment the data of the interface (i.e. the client) is sent to the server, which will carry out the simulation and return a volume for its visualization in panel in Fig. 2-g. A more advanced visualization can be obtained by pressing the button in Fig. 2-h; this action opens the panel shown

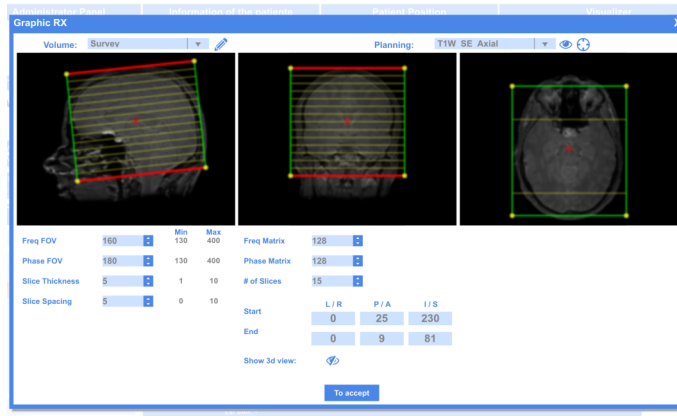


Fig. 3 Geometrical planning interface. This panel pops up when the “Graphic RX” button is pressed (see Fig. 2-k) and allows an interactive spatial location of the slices by means of rotation (yellow dots), the increase in the number of slices (red lines) and the displacement (red dot) of the area to be acquired. The remaining parameters can be set manually from the inputs of the panel. This planning can be done on any of the previously acquired slices that can be selected from the *Volume* drop-down. In addition, other planning previously carried out can be loaded using the *Planning* drop-down.

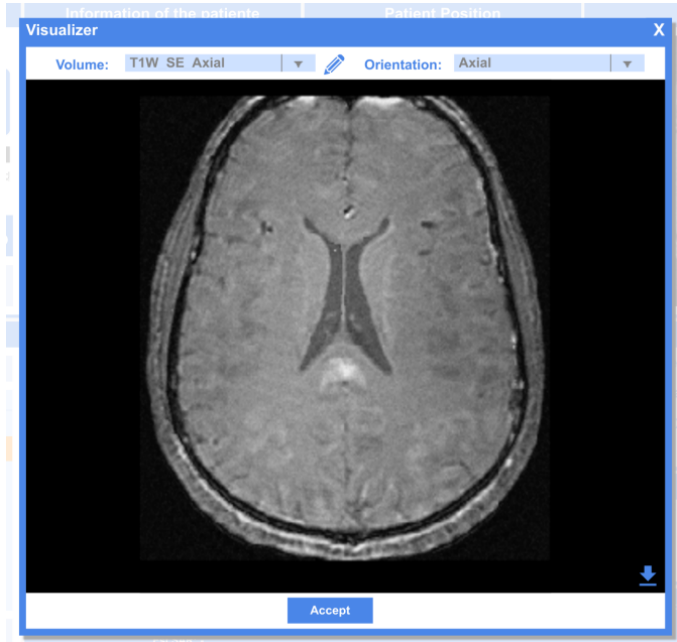


Fig. 4 Visualization panel. This panel pops up when the button in Fig. 2-h is pressed. The user can view all acquired slices in detail and, if desired, download them using the arrow located at the bottom of the image. Mouse interactions (zoom in and out, brightness/contrast and slice selection) are allowed.

in Fig. 4, from which acquired images can also be downloaded. All these visualizers allow interactions with the mouse to zoom in or zoom out, modify the brightness or contrast and move through the different slices acquired.

Some other panels offer additional functionality; this is the case of 2-e, where imaging options such as a *no phase wrap* acquisition or a *shimming* procedure can be selected.

Finally, following the requirements enumerated in section 2.1, we have included a panel to activate/deactivate different image artifacts, to select different hardware properties (field strength or field inhomogeneity, for instance), and to choose a specific case to be simulated (different anatomical regions and/or different pathologies). Most of these utilities are accessible using the panel in Fig. 2-a.

2.3.2 Geometrical planning

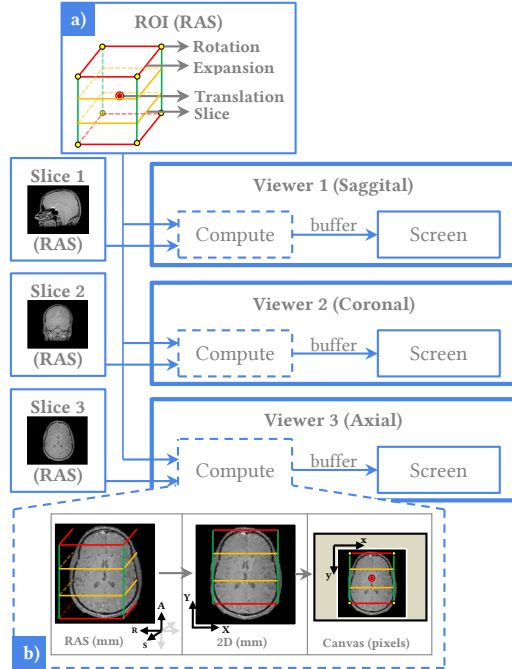


Fig. 5 Geometrical planning implementation. a) The region of interest (ROI) containing the 3D information of the slices will be shared through the different 2D viewers. In addition, each of the viewers will also be given an acquired slice with its corresponding 3D information. The viewer will take both inputs and calculate (block “Compute”) the projection of the ROI on the slice, while the information is stored in a buffer. When the block task is performed, the resulting image is drawn on the screen. b) indicates the necessary coordinate change from RAS (right-anterior-superior coordinate system.) to the pixels of the display.

Fig. 5 provides an overview on the geometrical planning. Let us denote by region of interest (ROI) the 3D hexahedral region that will contain the slices position to be acquired (see Fig. 5 a)). 3D planning is carried out by means of projecting the ROI on the 2D views, moving these projections by interface interactions in 2D and keeping track of these changes back in 3D. The ROI is shared between three components (the viewers) together with the images shown in the three of them. Coordinate exchange between the patient coordinate system (referred to as RAS in Fig. 5) and the image coordinate system and viceversa is constantly performed. The XTK library [27] provides support for all these operations through the controller.

To the best of our knowledge, this versatile planning tool has not been reported in any MRI simulator so far.

2.3.3 Simulation overview

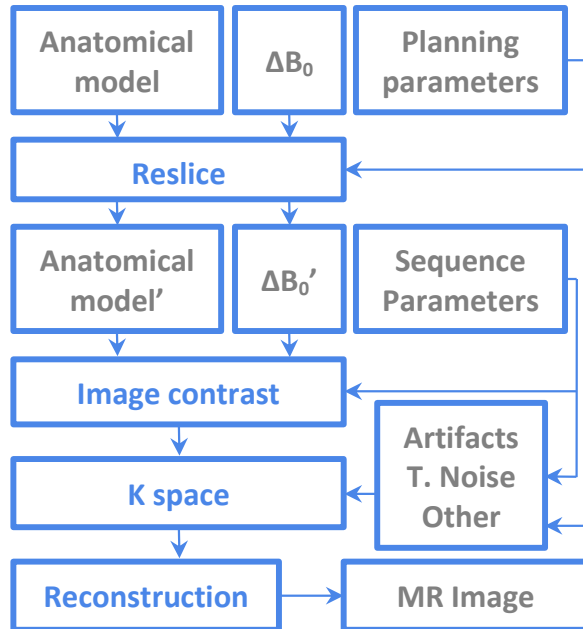


Fig. 6 Block simulation scheme shows the pipeline of the processing steps required for the computation of the simulated MRI images. The image is calculated in four steps: Adaptation of the volumes to the acquisition zone (Reslice); Calculation of the contrast image (Image contrast); Compute of the k-space and the artifacts (K space); And reconstruction of the image (Reconstruction).

Fig. 6 shows the processing steps followed for the computation of the simulated MRI images. The inputs are an *anatomical model*, the inhomogeneity magnetic field (ΔB_0), the geometrical *planning parameters* and the *sequence parameters*. The user selects one *anatomical model* among those offered by the simulator –head, neck, ankle, knee or a torso intended for cardiac planning–, each of them is a set of 3D volumes that contain the tissue properties needed for MR simulation, namely, proton density (PD), longitudinal relaxation time (T1) and transverse relaxation time (T2). They have been obtained from a real MR equipment using relaxometry sequences [28] with submillimetric resolution (within the range between 0.5 through 1mm, approximately isotropic). This will limit the actual spatial resolution of our simulations albeit arbitrarily small voxel sizes can be reconstructed. Other anatomical models are used depending on the simulation, such as ADC (Apparent Diffusion coefficient) in DWI (Diffusion Weighted Imaging) acquisitions. As for ΔB_0 , this is currently just a constant field that only affects the contrast of the image—a T2* weighting is obtained in gradient echo sequences—and, consequently, the signal to noise ratio is modified as well. This is intended to highlight the need of a shimming procedure prior to the actual acquisition (a self calibration to homogenize the field).

Geometrical *planning parameters* are specified by the user in the planning stage and they determine both the resolution and the FOV of the image. The *sequence parameters* are those specified in section 2.1.

Starting from the *anatomical model* and ΔB_0 , a reslice operation is first performed, which creates volumes of the size and properties specified by the user by means of the geometrical planning parameters. Next, image contrast is simulated from these volumes by evaluating the algebraic expression of the specific sequence [29] [30]. Afterwards, a Fourier transform is applied to the contrast image, yielding the so-called k-space. In this space, a number of artifacts can be easily simulated, such as motion effects, spike or thermal noise. In addition, attenuation effects from fast sequences are also incorporated, together with any other k-space manipulation options (half Fourier reconstruction, for instance). Finally, the inverse Fourier transform is computed to generate the resulting simulated MR image. This image will also contain additional spatial information (orientation, origin and voxel size) for its correct visualization.

3 Experimental work

3.1 Experiences

The MRI simulator has been employed in two experiences:

- An online course organized by the SERAM in May-July 2018. It included video lectures, with embedded slides to provide graphical support. The MRI simulator was employed as a complementary tool. Students were provided with a short video on how to use the simulator and then a small

number of exercises were given to illustrate its functionality. A total of 179 students participated in the online course.

- A one-day classroom experience with 32 students, carried out at the school of radiographers of Hospital San Carlos, Madrid, Spain, in October 29th, 2018. A 90-minute introductory session was given and a 90-minute hands-on workshop was then carried out, where the students were able to perform a series of specific tasks on the MRI simulator.

It is worth noting that the simulator was improved in several aspects from the first to the second experiment, incorporating new functionality. The descriptions in this paper refer to the updated version used for this second experiment.

3.2 Methods

Following industry standards, the System Usability Scale (SUS) [31] was employed to measure the usability of the MRI simulator. SUS is a 10-item five-point Likert scale that provides an overall usability score ranging from 0 to 100. Interestingly, SUS can be decomposed into two subscales [32], one composed of 8 items focusing on usability and the other with 2 items devoted to learnability. These subscales provide scores that can also be reported in the range of 0 to 100. Students were asked to answer the SUS questionnaire after the completion of their educational experience. In addition, participants were asked their Likelihood to Recommend (LTR) the MRI simulator to a user with a similar need (i.e. a prospective student of the same course) using a 5-point Likert-type item. LTR is highly correlated with SUS and can thus serve as a means for validation [33]. A last questionnaire was employed to measure the simulator perceived usefulness. It consists of two questions, namely: Q1) Was using the MRI simulator useful to learn concepts related to the principles of MRI? and Q2) Was using the MRI simulator useful to learn concepts related to MRI acquisition?. As in the LTR case, answers consisted of 5-point Likert-type items.

For the descriptive analysis, mean and standard deviation (SD) were used. For completeness, an inferential analysis was performed using a unpaired unilateral t-test, where the alternative hypothesis is “the mean of the *Classroom Experiment* is greater than the mean of the *Online Course*”; the null hypothesis is considered rejected whenever the p-value is smaller than 0.05.

3.3 Results

A total of 116 and 29 responses were respectively collected from each experience. In both cases, the number of responses is above the commonly accepted minimum of 12 [34].

Table 1 shows the results of the SUS and the LTR; the first two columns indicate the values of SUS overall parameter, its two subscales and the LTR (mean \pm SD). In the two educational experiences, SUS results fall within the

Table 1 Statistical analysis of SUS and LTR. Mean, standard deviation (SD) and the unpaired t-test are computed. T-test return the p-value of the alternative hypothesis that mean of the *Classroom Experiment* is greater than the mean of the *Online Course*.

		Online Course (Mean \pm SD)	Classroom Experiment (Mean \pm SD)	t-test right tail (p-value)
SUS	Overall	55.86 \pm 20.59	63.02 \pm 13.39	0.0389
	Usability	59.78 \pm 22.42	67.03 \pm 14.09	0.0497
	Learnability	40.19 \pm 25.63	46.98 \pm 27.27	0.1050
	LTR	3.65 \pm 1.23	4.45 \pm 0.63	0.0005

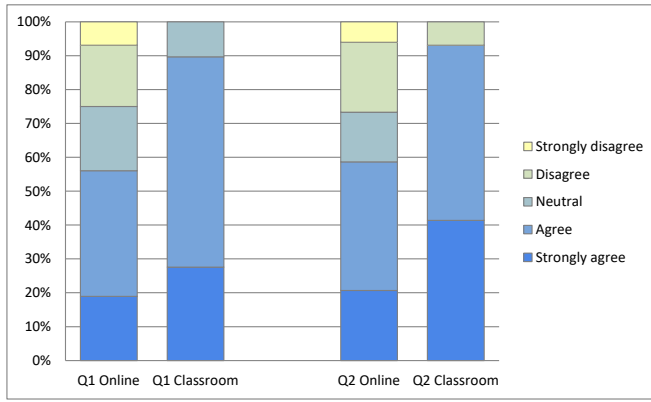


Fig. 7 Perceived usefulness to learn principles (Q1) and acquisition (Q2) of MRI using the simulator. The graph compares the results of questions Q1 and Q2 obtained in both experiences.

“Ok” range according to [35]. In addition, the LTR values indicate that most of the students would recommend our simulator to their peers; notice that the maximum value of LTR in the scale we have used is 5.

Some differences between the two experiences can also be observed. Results are shown in the last column of the table, where we show the p-value of a right-sided t-test. Statistical differences have been obtained in three out of the four parameters we have measured. This essentially means that the lessons learnt with the first educational experience let us improve the quality of our teaching with the tool. Additional considerations are provided in the next section.

Figure 7 shows the results of perceived usefulness. In both educational experiences most of the students provide a positive answer for the two questions, especially for the Q2, which is directly related to image acquisition. In comparative terms, differences between the two experiences have been observed, with p-values < 0.001 in both questions.

4 Discussion

We have identified several features that are, in our opinion, essential for the simulator to be a useful tool in realistic learning scenarios. To the best of our knowledge some of these features, such as the ability to perform 3D geometrical planning, the capacity to create and customize not only acquisition sequences but also protocols, and the existence of different roles in a web-based application, have not been proposed before in the literature.

Several conclusions can be extracted from the results in the previous section. The main conclusion is that a simulator built upon the functional and non-functional requirements we have identified is indeed perceived by most of the students as a useful tool for learning concepts related to MRI and it is likely that they will recommend it to their peers. Some additional conclusions can also be reached. First, user satisfaction has increased notably from the first to the second experiment, as indicated in section 3.3. Two factors contribute to this increase, (a) improvements were incorporated into the simulator for the second experiment, including some additional functionality, bug correction and overall robustness, and mainly (b) the amount of specific training on the use of the simulator increased: for the first experiment, only a 19-minute video was available while, for the second experiment, on-site guidance about the use of the simulator was provided. This probably indicates that a significant amount of training on the use of the simulator is needed before the user is able to exploit its capabilities.

Second, good results were obtained, especially in the second experiment, concerning perceived usefulness (Fig. 7). Thus, students find the simulator interesting as long as they receive sufficient training on the use of the simulator.

Third, as previously stated, the overall SUS score obtained in both experiences (Table 1) was rated as “OK”. Interestingly, higher overall scores were not achieved because the learnability score was somewhat low, which suggests the idea that students had some difficulties to learn how to use the MRI simulator. The LTR scores are in line with the corresponding SUS scores. We maintain, however, that a MR simulator should not unrealistically simplify the usage of such a system, but rather mimic it so that trainees can eventually apply the acquired knowledge in realistic scenarios. Sufficient training to use the simulator, as previously stated, seems mandatory.

Our current tool has a number of limitations. Specifically, the proposed simulation strategy, which consists in using the analytical expression of the sequence for generating the MRI signal, does allow quick interaction with the user. Nevertheless, this means that the generation of artifacts has to be imposed, as it is the case with noise, chemical shift or fold-over effects. But those artifacts due to more complex MRI phenomena such as eddy currents, off-resonance effects, slice profile imperfections, stimulated echoes and many others are not so straightforward, so simulated images may not always be realistic. However, thanks to the client-server architecture, more sophisticated simulation paradigms, including those that show specific computing needs such

as graphical processing units (GPUs), can be integrated into the system while leaving the client unaltered or only slightly modified.

In addition, the application is currently limited to basic sequences as well as to a reduced number of anatomies; however, the addition of new anatomies, including cases with different pathologies, only requires the acquisition of the images necessary for the simulation.

We have meant to be vendor agnostic; nevertheless, each MRI vendor shows specific GUI designs as well as trade names for the sequences, which may require targeted training. However, bearing in mind the MVVM architecture, our tool is indeed prepared to create secondary GUIs in which both aesthetics and nomenclature changes should be easily accommodated.

5 Conclusions and future work

We have presented an MRI simulation tool, designed for educational purposes, that emulates the pipeline that an MRI operator performs to carry out image acquisitions in clinical practice. The system has been designed on the basis of a number of functional and non functional requirements that have proven useful to facilitate the learning process, including resemblance with an actual MRI console and the capacity to perform sequence and protocol creation, parameter adjustment, 3D geometrical planning and possible activation or deactivation of acquisition artifacts.

Web technology was employed to guarantee ubiquitous access; also, complexity in the client side has been kept to a minimum, and involved calculations are carried out in the server side. This greatly facilitates the addition of functionality.

The simulation tool has been used in two real educational experiences. Based on the collected quantitative parameters, we can conclude that the proposed system is a valuable educational tool for training in MRI principles and acquisition.

Acknowledgments

This work has been funded in part by the Junta de Castilla y León, Spain, and by the company Giveme5D, Valladolid, Spain. The authors would like to thank the SERAM, the Hospital San Carlos as well as Fátima Matute, MD, and Prof. José Ramón Casar Corredera, PhD, for their invaluable help to carry out the educational experiments. We also acknowledge grant TEC2017-82408-R.

Compliance with Ethical Standards

This work has been carried out at the University of Valladolid and has been partially funded by the company Giveme5D, Valladolid, Spain. A technology transfer agreement has been signed by both parties. The second author is

the main shareholder of this company; he has provided radiological guidance throughout the simulator design process.

All information related to the tests described in the paper was obtained anonymously and with the participants consent to use this information for research purposes.

References

1. Robert R Edelman. The history of mr imaging as seen through the pages of radiology. *Radiology*, 273(2S):S181–S200, 2014.
2. Muhammed E and Azim Ç. *MRI Handbook*. Springer-Verlag New York, Yeni Yüzyıl University, Cevizlibağ Topkapi, Turkey, 1 edition, 2012.
3. Noz ME, Erdman WA, Maguire GQ, Stahl TJ, Tokarz RJ, Menken KL, and Salviani JA. Modus operandi for a picture archiving and communication system. *Radiology*, 152(1):221–223, 1984.
4. Huang HK. Three methods of implementing a picture archiving and communication system. *RadioGraphics*, 12(1):131–139, 1992.
5. Hagmann P, Jonasson L, Maeder P, Thiran JP, Wedeen VJ, and Meuli R. Understanding diffusion mr imaging techniques: From scalar diffusion-weighted imaging to diffusion tensor imaging and beyond. *RadioGraphics*, 26(suppl_1):S205–S223, 2006.
6. Geir Torheim, Peter A. Rinck, Richard A. Jones, and Jørn Kvaerness. A simulator for teaching mr image contrast behavior. *Magnetic Resonance Materials in Physics, Biology and Medicine*, 2(4):515–522, Dec 1994.
7. Hackländer T and Mertens H. Virtual mri: A pc-based simulation of a clinical mr scanner. *Academic radiology*, 12:85–96, Feb 2005.
8. Jochimsen TH and von Mengerhausen M. Odin - object-oriented development interface for nmr. *Journal of magnetic resonance*, 170:67–78, 10 2004.
9. Stöcker T, Vahedipour K, Pflugfelder D, and Shah NJ. Highperformance computing mri simulations. *Magnetic Resonance in Medicine*, 64(1):186–193, 2010.
10. Cao Zhipeng, Oh Sukhoon, Sica Christopher T, McGarry John M., Horan Timothy, Luo Wei, and Collins Christopher M. Blochbased mri system simulator considering realistic electromagnetic fields for calculation of signal, noise, and specific absorption rate. *Magnetic Resonance in Medicine*, 72(1):237–247, 2013.
11. Santiago Aja-Fernndez, Gonzalo Vegas-Snchez-Ferrero, and Antonio Tristn-Vega. Noise estimation in parallel mri: Grappa and sense. *Magnetic Resonance Imaging*, 32(3):281 – 290, 2014.
12. Drobniak I, Gavaghan D, Süli E, Pitt-Francis J, and Jenkinson M. Development of a functional magnetic resonance imaging simulator for modeling realistic rigid-body motion artifacts. *Magnetic Resonance in Medicine*, 56:364–80, 08 2006.
13. Christos G Xanthis, Ioannis E Venetis, and Anthony H Aletras. High performance mri simulations of motion on multi-gpu systems. *Journal of Cardiovascular Magnetic Resonance*, 16(1):48, Jul 2014.
14. Gregorio Andria, Filippo Attivissimo, Giuseppe Cavone, and Anna Maria Lucia Lanzolla. Acquisition times in magnetic resonance imaging: Optimization in clinical use. *IEEE Transactions on Instrumentation and Measurement*, 58(9):3140–3148, Sept 2009.
15. Hansen MS and Sørensen TS. Gadgetron: An open source framework for medical image reconstruction. *Magnetic Resonance in Medicine*, 69(6):1768–1776, 2012.
16. Zwart NR and Pipe JG. Graphical programming interface: A development environment for mri methods. *Magnetic Resonance in Medicine*, 74(5):1449–1460, 2014.
17. Martin Uecker, Frank Ong, Jonathan I Tamir, Dara Bahri, Patrick Virtue, Joseph Y Cheng, Tao Zhang, and Michael Lustig. Berkeley advanced reconstruction toolbox. In *Annual Meeting of the International Society for Magnetic Resonance in Medicine*, In Proc. Intl. Soc. Mag. Reson. Med., page 2486, 2015.
18. Drobniak I, Pell GS, and Jenkinson M. Simulating the effects of time-varying magnetic fields with a realistic simulated scanner. *Magnetic Resonance Imaging*, 28(7):1014 – 1021, 2010.

19. Graham MS, Drobniak I, and Zhang H. Realistic simulation of artefacts in diffusion mri for validating post-processing correction techniques. *NeuroImage*, 125:1079 – 1094, 2016.
20. Graham MS, Drobniak I, Jenkinson M, and Zhang H. Quantitative assessment of the susceptibility artefact and its interaction with motion in diffusion mri. *PLOS ONE*, 12(10):1–25, 10 2017.
21. Benoit-Cattin H, Collewet G, Belaroussi B, Saint-Jalmes H, and Odet C. The simri project: a versatile and interactive mri simulator. *Journal of Magnetic Resonance*, 173(1):97 – 115, 2005.
22. Xanthis CG, Venetis IE, Chalkias AV, and Aletras AH. Mrisimul: A gpu-based parallel approach to mri simulations. *IEEE Transactions on Medical Imaging*, 33:607–617, 2014.
23. Ryoichi Kose and Katsumi Kose. Blochsolver: A gpu-optimized fast 3d mri simulator for experimentally compatible pulse sequences. *Journal of Magnetic Resonance*, 281:51 – 65, 2017.
24. Fang Liu, Julia V. Velikina, Walter F. Block, Richard Kijowski, and Alexey A. Samsonov. Fast realistic mri simulations based on generalized multi-pool exchange tissue model. *IEEE Transactions on Medical Imaging*, 36(2):527–537, Feb 2017.
25. Chris Anderson. *The Model-View-ViewModel (MVVM) Design Pattern*, pages 461–499. Apress, Berkeley, CA, 2012.
26. Carl Burch. Django: a web framework using python: Tutorial presentation. *Journal of Computing Sciences in Colleges*, 25(5):154–155, May 2010.
27. Hähn D, Rannou N, Ahtam B, Grant PE, and Pienaar R. Neuroimaging in the browser using the x toolkit. In *Proceedings of the 5th INCF Congress of Neuroinformatics*, Munich, Germany, 2012.
28. G. Ramos-Llordén, A J. den Dekker, G. Van Steenkiste, B. Jeurissen, F. Vanhevel, J. Van Audekerke, M. Verhoye, and J. Sijbers. A unified maximum likelihood framework for simultaneous motion and t1 estimation in quantitative MR t1 mapping. *IEEE Trans Med Imag*, 36(2):433–466, 2017.
29. Paul C. Lauterbur Zhi-Pei Liang. *Principles of magnetic resonance imaging: a signal processing perspective*. IEEE Press Series on Biomedical Engineering, 2000.
30. Matt A. Bernstein, Kevin F. King, and Xiaohong Joe Zhou, editors. *Handbook of MRI Pulse Sequences*. Academic Press, Burlington, 2004.
31. Jhon Brooke. Sus: A quick and dirty usability scale. *Usability Eval. Ind.*, 189, 11 1995.
32. James R. Lewis and Jeff Sauro. The factor structure of the system usability scale. In Masaaki Kurosu, editor, *Human Centered Design*, pages 94–103, Berlin, Heidelberg, 2009. Springer Berlin Heidelberg.
33. James R. Lewis. Usability: Lessons learned and yet to be learned. *International Journal of HumanComputer Interaction*, 30(9):663–684, 2014.
34. Thomas S. Tullis and Jacqueline N. Stetson. A comparison of questionnaires for assessing website usability. In *Usability Professionals Association (UPA) 2004 Conference*, Jun 2004.
35. Aaron Bangor, Philip Kortum, and James Miller. Determining what individual sus scores mean: Adding an adjective rating scale. *J. Usability Studies*, 4(3):114–123, May 2009.